Wiley
Advances in Meteorology
Volume 2025, Article ID 4732468, 16 pages
https://doi.org/10.1155/adme/4732468

WILEY

Research Article

Impact of the Suspension of a Metallurgical Complex: SO_2 Analysis and Vegetation Restoration Through Remote Sensing

Deyvis Cano[1], **Richard Peñaloza**[2], **Carlos Cacciuttolo**[3], **Tatiana Mora Kuplich**[4,5], **Dámaso W. Ramírez**[6] and **Luis Suárez-Salas**[7]

[1]*Academic Program of Environmental Engineering, Universidad de Huánuco, Huánuco, Peru*
[2]*Faculty of Animal Science, Universidad Nacional del Centro del Perú, Huancayo, Peru*
[3]*Department of Civil Engineering, Universidad de Castilla-La Mancha, Ciudad Real, Spain*
[4]*Postgraduate Program in Remote Sensing, Universidade Federal do Rio Grande do Sul, Porto Alegre, Rio Grande do Sul, Brazil*
[5]*Earth Observation and Geoinformatics Division, National Institute for Space Research, São José dos Campos, Brazil*
[6]*Faculty of Environmental Sciences, Universidad Científica del Sur, Lima, Peru*
[7]*Instituto Geofísico del Perú, Lima, Peru*

Correspondence should be addressed to Deyvis Cano; deyvis.cano@udh.edu.pe

Received 8 February 2025; Revised 18 August 2025; Accepted 2 September 2025

Academic Editor: Antonio Donateo

Sulfur dioxide (SO_2) pollution significantly threatens ecosystems and public health, particularly in highly industrialized regions. This study evaluates the impact of suspending activities at the La Oroya Metallurgical Complex (CMLO, by its Spanish acronym), one of the most relevant historical sources of SO_2 pollution in the Central Andes of Peru. Using remote sensing data (MODIS and Ozone Monitoring Instrument [OMI]), temporal and spatial trends in the normalized difference vegetation index (NDVI) and SO_2 concentrations were analyzed from 2000 to 2019. The results show an average reduction of 82.18% in SO_2 after the CMLO was stopped, accompanied by a significant positive increase in the NDVI trend ($p < 0.05$), which shows a recovery of the vegetation in surrounding areas. Vegetation regeneration showed marked spatial patterns to the southwest and southeast of the CMLO, influenced by the dispersion of pollutants through prevailing winds. However, the moderate relationship between the decrease in SO_2 and NDVI ($R^2 = 0.10$) suggests the influence of additional factors, such as the historical accumulation of heavy metals, water scarcity, and the specific characteristics of high Andean soils and vegetation.

Keywords: aerosols; biomonitoring; ecotoxicology; mining; plant resilience; smelting; vegetation regeneration

1. Introduction

Atmospheric pollution by sulfur dioxide (SO_2) is a serious public health and environmental issue [1]. This pollutant primarily originates from industrial processes, vehicle emissions, and volcanic sources [2]. Additionally, SO_2 is a precursor to fine particles (particulate matter [PM]2.5), significantly affecting respiratory health [3]. SO_2 contributes to acid rain formation, damaging aquatic ecosystems, soils, and structures [4]. It also influences climate change by affecting aerosol formation, which, in turn, impacts solar radiation and the thermal balance of the atmosphere [5].

Plants have efficiently absorbed, accumulated, and regulated atmospheric SO_2 [6]. Vegetation effectively reduces air pollutant concentrations, including PM, nitrogen oxides (NO_x), and SO_2, with notable reductions in these pollutants [7, 8]. Studies indicate that after reducing SO_2 emissions, plants can recover their normal levels within one or two growing seasons [9]. This vegetation recovery can be monitored using remote sensing at different spatial and temporal scales, employing spectral indices like the normalized difference vegetation index (NDVI) [10]. Additionally, remote sensing can assist with estimating key vegetation properties, such as productivity and leaf area index (LAI), which are crucial for

analyzing large-scale vegetation changes in response to environmental factors related to climate and atmospheric alterations [11].

A notable case of SO_2 pollution is the city of La Oroya, located in the Central Andes of Peru and known as Latin America's first metallurgical city. La Oroya has been categorized as one of the most polluted cities in the world [12]. In 2009, the Peruvian state suspended the activities of the La Oroya Metallurgical Complex (CMLO) due to noncompliance with environmental standards under the Environmental Remediation and Management Program (PAMA) [13]. The surrounding area consists of high-altitude ecosystems with sparse vegetation, mainly composed of natural grasslands and remnants of shrublands, attributed to the accumulation of heavy metals and toxic gases such as SO_2 since 1922 [14]. Currently, part of the population of La Oroya, the central government, and some private companies are making efforts to reactivate the CMLO despite ongoing social and environmental conflicts, focusing mainly on aspects that promote the city's economic development [15]. However, there is a substantial concern that if these efforts succeed, the public health and environmental situation, particularly in surrounding areas, may not be adequately considered, as there is no large-scale territorial diagnosis on the impact of these pollutants on ecosystems, especially vegetation [16].

Given this situation, it is crucial to assess the degree of degradation and recovery of vegetation in this SO_2-polluted environment, which will help understand the effects of this pollutant on vegetation in these ecosystems. In this context, the present study aims to evaluate the impact of the suspension of activities at the Metallurgical Complex on vegetation regeneration near the CMLO and the spatial and temporal dynamics of the atmospheric pollutant SO_2, using remote sensing. The analysis will evaluate the NDVI trend for vegetation over 2000–2019 and SO_2 over 2005–2019. Additionally, a temporal relationship analysis between NDVI and SO_2 will be conducted to assess the extent of this pollutant's impact on vegetation. This information is expected to help consider the effects of pollution from this mining-metallurgical industry, as it is associated with underlying conflicts between economic, social, and environmental aspects.

2. Materials and Methods

2.1. Study Area. La Oroya is in the Junín region, in the central part of Peru, approximately at 11.52°S latitude and 75.90°W longitude. Known as the first metallurgical city in Latin America, La Oroya has unfortunately been classified as one of the most polluted cities in the world. It is situated 3745 m above sea level (Figure 1). It has two well-defined climatic seasons: the dry season (from May to September) and the rainy season (from October to April), with an average annual accumulated precipitation of 1374 mm. Temperatures range between 2 and 12°C on average. La Oroya is a commercial city that is economically dependent on mining and livestock farming and has developed in adjacent districts. Steep and rocky hills with sparse vegetation characterize the surroundings. However, nearby areas feature vegetation from high Andean ecosystems, including grassland communities and remnants of shrublands dominated by species such *as Festuca dolichophylla*, *Stipa ichu*, and *Stipa obtusa*.

According to the global atmospheric reanalysis MERRA-2 (Modern-Era Retrospective Analysis for Research and Applications, Version 2), developed by NASA through the Global Modeling and Assimilation Office (GMAO), using data from the POWER Project Release 8 (available at: https://power.larc.nasa.gov/data-access-viewer/), the winds in the CMLO study area in La Oroya, reported during the year 2019, are characterized as being relatively fast, with an average speed of 3.17 m/s (Figure 2a). The predominant wind direction is from northeast to southwest, with 24% of the time having wind speeds ranging from 0.50 to 8.80 m/s (Figure 2b). Likewise, higher speeds occur during the day, prevailing 36% of the time in the range of 3.60–8.80 m/s, while at night the winds are lighter, with speeds from 0.50 to 5.70 m/s, occurring between 8% and 16% of the time (Figure 2c). These dynamics are influenced by daily temperature variations (annual average $= 9.24 \pm 4.09$°C) and, consequently, by changes in atmospheric pressure (average of 100.71 ± 0.62 kPa; Figure 2a). Analyzing the wind during the dry and rainy seasons shows no significant differences.

These data sources, mentioned above, were used to determine the wind flow and direction for the nearby cities analyzed in this study.

2.2. NDVI and SO_2 Data. Vegetation data were obtained from the NDVI monthly MODIS Terra images of the MOD13A3 version 6.1 product, with a spatial resolution of 1 km. This index is ideal for this location as it is not likely to saturate due to the sparse vegetation. By generating this monthly product, the algorithm incorporates all overlapping MOD13A2 products for the month and uses a weighted temporal average. Vegetation indices are used for global monitoring of vegetation conditions and are included in products that display land cover and its changes. These data can serve as inputs for modeling global biogeochemical and hydrological processes and global and regional climate. This product is available on Google Earth Engine (GEE; available at: https://developers.google.com/earth-engine/datasets/catalog/MODIS_061_MOD13A3).

SO_2 data were obtained from the Ozone Monitoring Instrument (OMI), which has collected data since August 9, 2004. Total SO_2 monitoring (vertical column in Dobson units [DUs], where $1\ \text{DU} = 2.69 \times 10^{16}$ molecules/cm^2) is performed using the OMSO2e product at a grid resolution of 0.25° (~27.75 km). Each grid contains only one observation of the total SO_2 column density in the planetary boundary layer. This single observation is the "best pixel." This data is available on the Goddard Interactive Online Visualization and Analysis Infrastructure (GIOVANNI). This tool allows users to visualize, interact with, and analyze data from several NASA-supported missions (available at: https://giovanni.gsfc.nasa.gov/giovanni/).

2.3. NDVI and SO_2 Trend Analysis. The spatial and temporal data for NDVI and SO_2 were taken on dates with low cloud cover in the study area (April 11–October 14) during

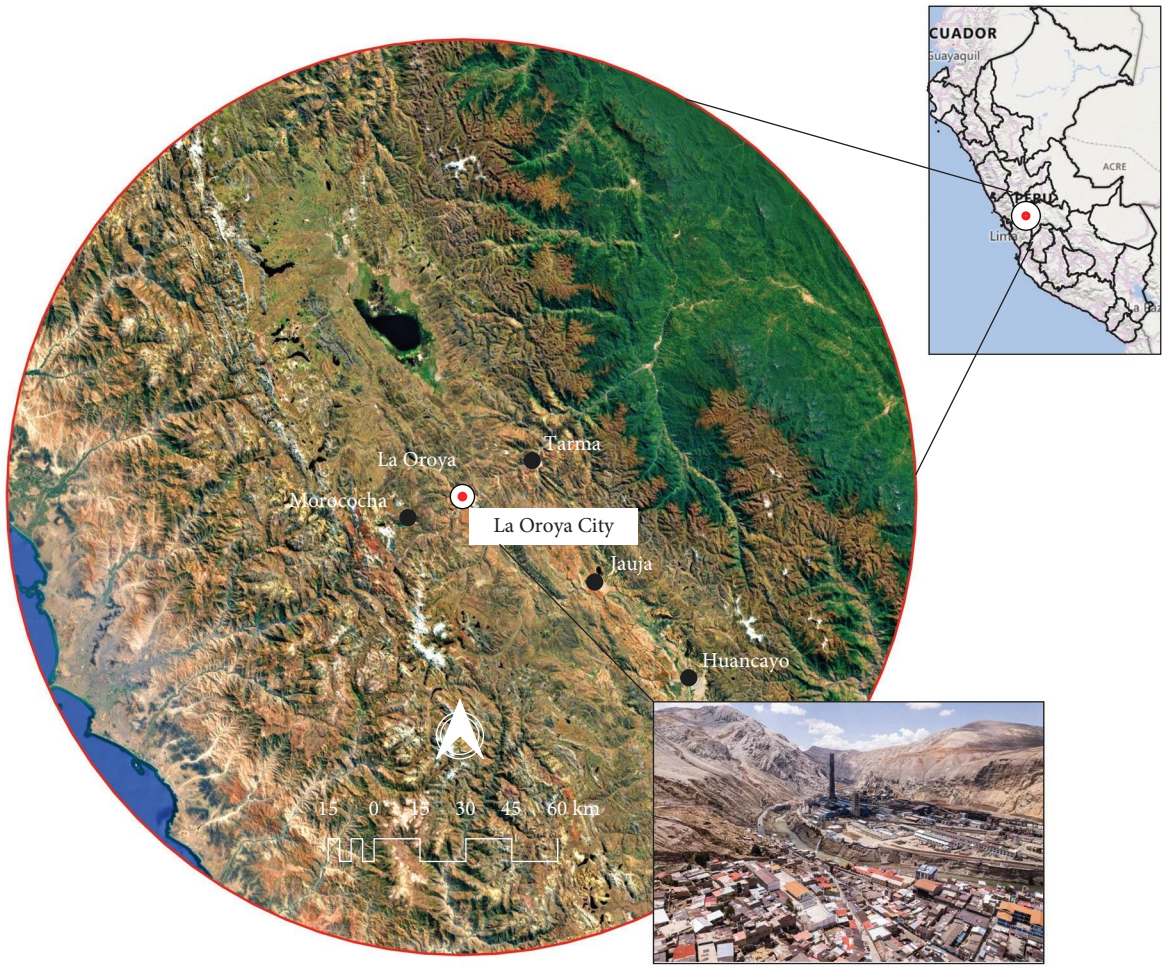

FIGURE 1: The study area is located in the metallurgical city of La Oroya and the surrounding cities.

2000–2019 for NDVI and 2005–2019 for SO_2, respectively, based on data availability. Additionally, the nonparametric Mann–Kendall trend test (S) was applied per pixel to detect the presence of an upward or downward trend in the data overtime [17]. This test has the advantage of being insensitive to outliers, focusing on value ranks rather than the values themselves. Moreover, it is suitable for small samples [18]. The equation is calculated as the Mann–Kendall correlation coefficient (S) and is configured as follows:

$$S = \sum_{i=1}^{n-1} \sum_{j=i+1}^{n} \operatorname{sign}(x_i - x_j), \tag{1}$$

where n is the number of data points, x_i and x_j are the data values in the time series when $j > i$. The sign $(x_i - x_j)$ is interpreted according to its sign as follows:

$$\operatorname{sign}(x_i - x_j) = \begin{cases} +1 & \text{if } x_i - x_j < 0 \\ 0 & \text{if } x_i - x_j = 0 \\ -1 & \text{if } x_i - x_j > 0 \end{cases}. \tag{2}$$

The variance is calculated as follows:

$$\operatorname{VAR}(S) = \frac{n(n-1)(2n-5) - \sum_{i=1}^{m} t_i(t_i-1)(2t_i+5)}{18}, \tag{3}$$

where n is the number of data points, m is the number of tied groups, and t_i denotes the number of ties of length i. This helps evaluate data dispersion. The described procedure is used to calculate the Z-score to assess significance as follows:

$$Z = \begin{cases} \dfrac{S-1}{\sqrt{\operatorname{VAR}(S)}}, & \text{if } S > 0 \\ 0, & \text{if } S = 0 \\ \dfrac{S+1}{\sqrt{\operatorname{VAR}(S)}}, & \text{if } S < 0 \end{cases}. \tag{4}$$

This procedure was generated in GEE based on the code available at https://developers.google.com/earth-engine/tutorials/community/nonparametric-trends.

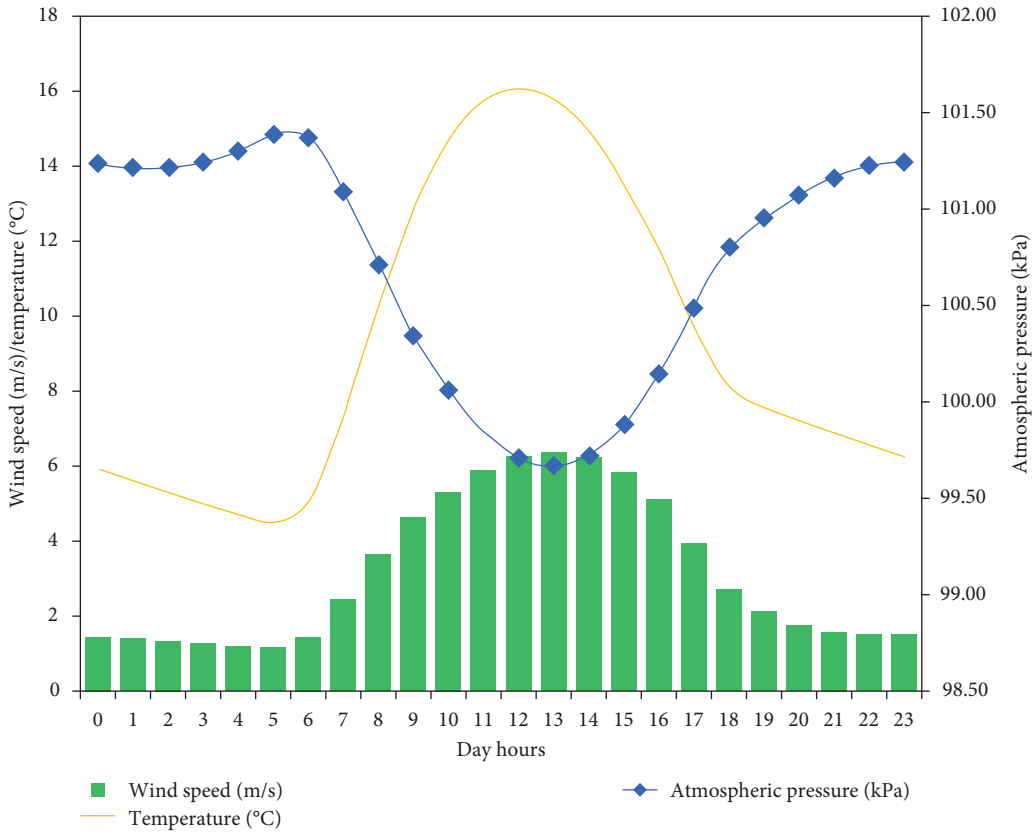

(a)

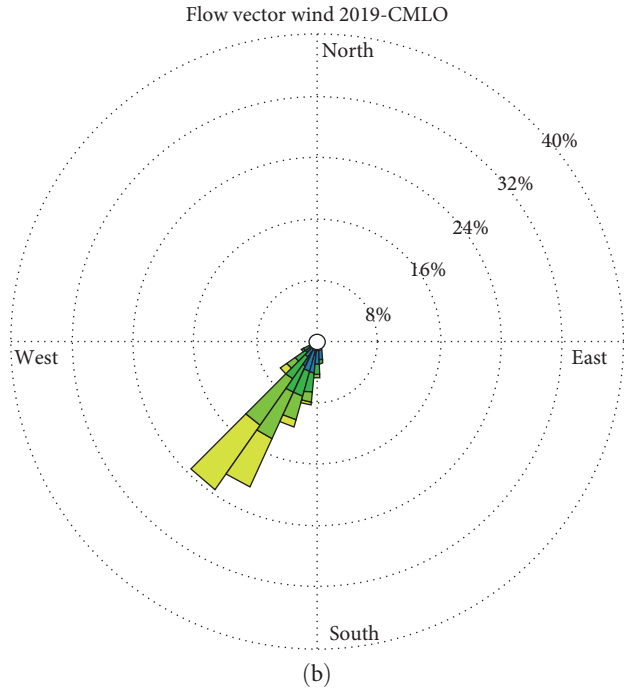

(b)

Figure 2: Continued.

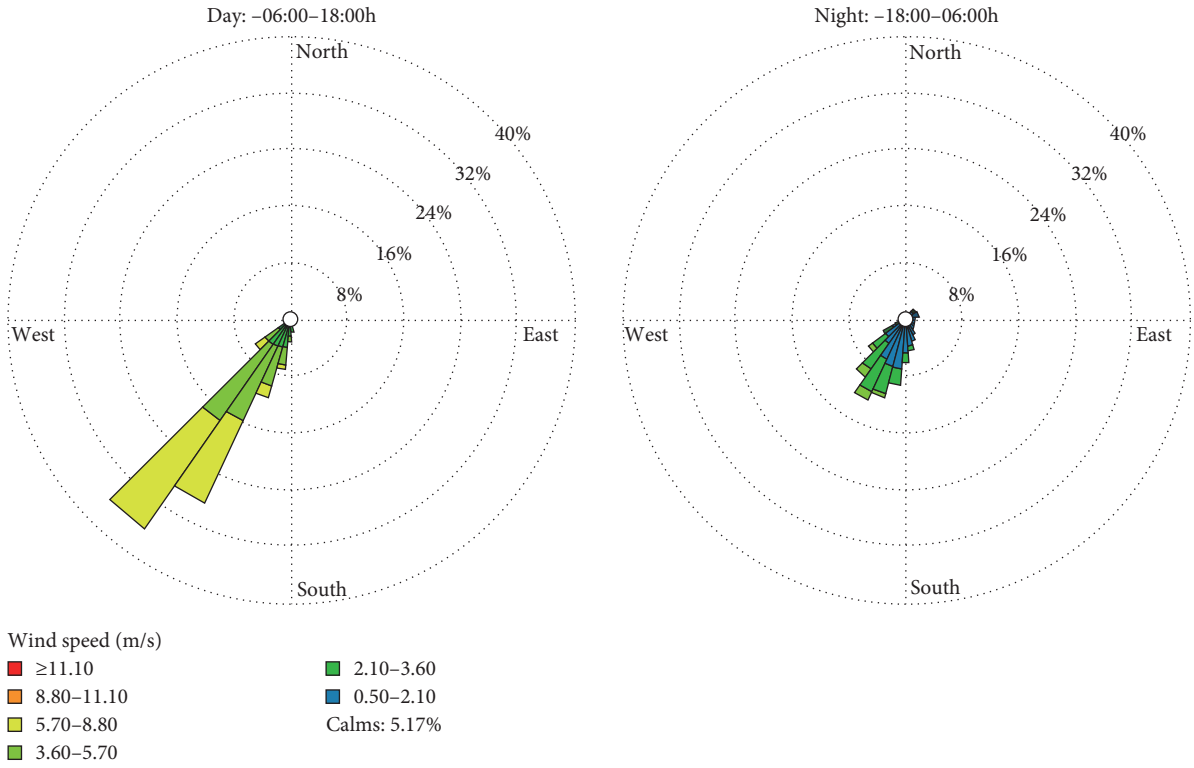

(c)

FIGURE 2: Hourly characteristics of wind, atmospheric pressure, and temperature at the SO_2 emission site of the CMLO during the year 2019. (a) Hourly variation of wind speed, atmospheric pressure, and temperature. (b) Wind rose with flow vectors indicating the direction toward which the wind is blowing and its speed. (c) Wind rose differentiated by time slots: daytime (06:00–18:00) and nighttime (18:00–06:00).

TABLE 1: Classification criteria for trends based on statistical significance.

MK value range	*Z* value range	*p*-Value	Category
$S>0$	$Z>2.58$	<0.001	Highly significant positive trend
	$1.96<Z\leq 2.58$	<0.01	Significant positive trend
	$1.65<Z\leq 1.96$	<0.05	Weakly significant positive trend
	$Z\leq 1.65$	<0.1	Nonsignificant trend
$S=0$	$Z=0$	>0.1	No change
$S<0$	$Z>2.58$	<0.001	Highly significant negative trend
	$1.96<Z\leq 2.58$	<0.01	Significant negative trend
	$1.65<Z\leq 1.96$	<0.05	Weakly significant negative trend
	$Z\leq 1.65$	<0.1	Nonsignificant trend

The operation results are grouped into nine categories (Table 1), according to the magnitude and direction of the trend. The restrictions are detailed: when $S>0$, a positive trend is identified; if $S<0$, the trend is negative; and if $S=0$, there is no change. Statistical significance is evaluated using the Z value: if $Z>2.58$, the trend is highly significant ($p<0.001$); between 1.96 and 2.58, significant ($p<0.01$); between 1.65 and 1.96, slightly significant ($p<0.05$); and if $Z\leq 1.65$, the trend is not significant ($p<0.10$) [19]. All these analyses were completed using QGIS software version 3.34.9.

2.4. Time Series Analysis. To analyze the daily time series of SO_2 during the 2005–2019 period, a rectangular study area of 100 km × 150 km was delineated, where a significant negative trend was observed. This polygon allowed for the average time series of all pixels within the defined area to be obtained using the GIOVANNI platform. Simultaneously, the monthly NDVI time series for the 2000–2019 period was analyzed to identify zones with a significant positive trend in vegetation.

High-resolution images were used to locate extensive areas of natural vegetation, mainly grasslands. A square of approximately 1 km^2 was delineated in these locations. These areas were selected near significant cities in the Junín region close to La Oroya, including La Oroya, Jauja, Tarma, Huancayo, and Morococha. All-time series data were obtained from GEE using MODIS Terra, product MOD13A3 version 6.1.

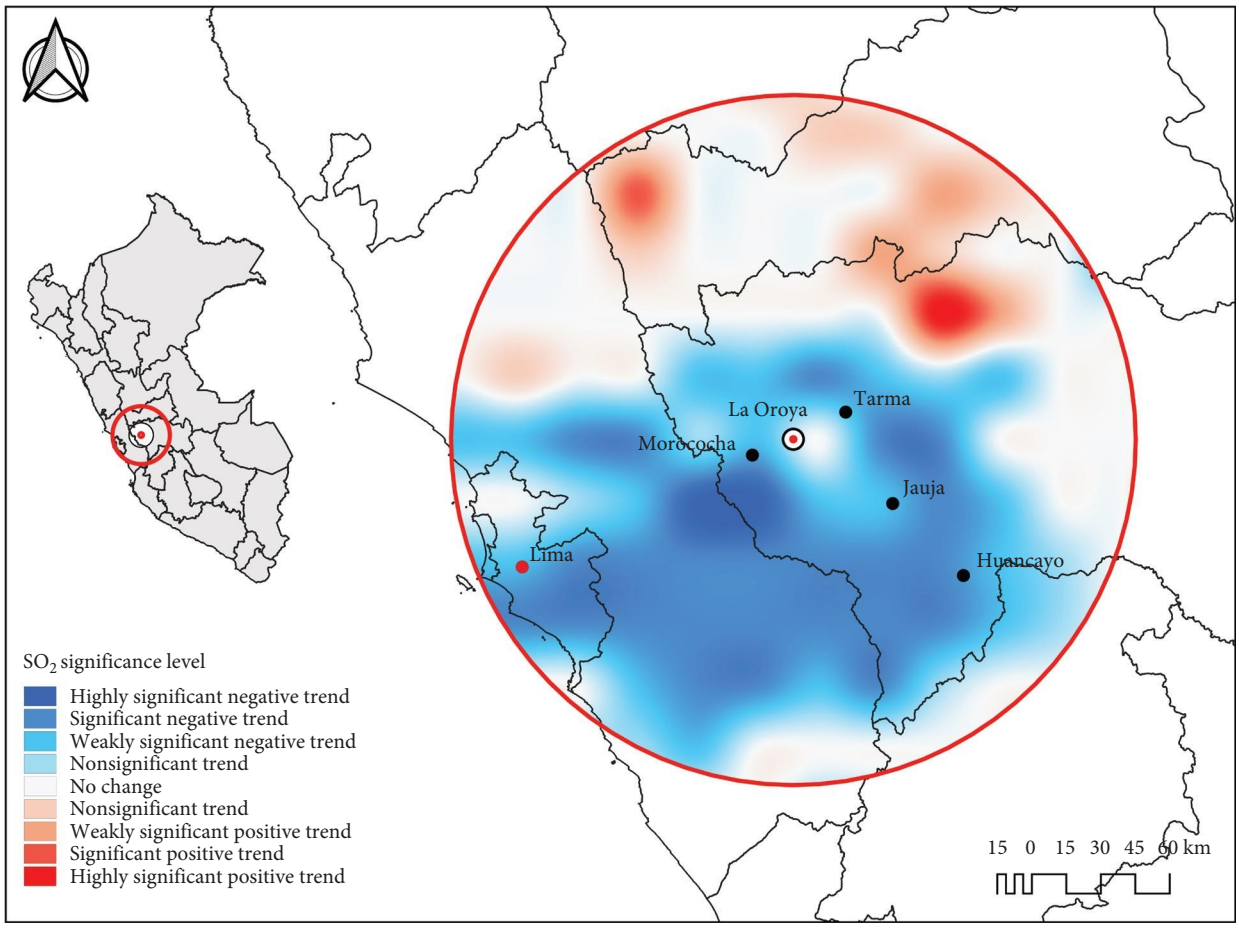

FIGURE 3: Significance levels of SO_2 trend in DU units.

The time series of both variables, SO_2 and NDVI, were divided into 2000–2009 and 2010–2019 for NDVI and 2005–2009 and 2010–2019 for SO_2. This division enabled a trend analysis and a comparison of means between periods before and after the shutdown of the CMLO. All analyses were conducted using QGIS software version 3.34.9 and MS Excel.

2.5. Field Monitoring Data of SO_2. Atmospheric monitoring data near the CMLO were used, collected between 1999 and 2024, through 3–4 casual monitoring campaigns per year, carried out in public spaces such as educational centers, healthcare facilities, homes, and other urban environments. These data are available on the Regional Health Directorate (DIRESA) portal, the regional health authority responsible for directing, implementing, and evaluating comprehensive health care policies, in coordination with the Ministry of Health (MINSA). The records are part of the National Air Quality Surveillance Program and can be consulted at the following link: http://www.digesa.minsa.gob.pe/DCOVI/mapas/DIGESA_AIR_MR_CalidadAirePuntual_JUNIN.html#SO2a. These data were collected by Supreme Decree Number 010-2019-MINAM, which approves the National Protocol for Environmental Air Quality Monitoring in Peru. This protocol defines standardized technical criteria to ensure the information generated is comparable, reliable, and representative. The data obtained allowed for the validation of annual SO_2 levels in $\mu g/m^3$ through a linear regression analysis, relating them with SO_2 data in DUs provided by the OMI sensor, using the coefficient of determination (R^2) and the mean absolute error (MAE) as indicators.

2.6. Statistical Analyses. The statistical analyses applied to the time series included the Mann–Kendall trend test at a 95% significance level to evaluate trends before and after the CMLO shutdown. Additionally, a comparison of means was conducted using the Student's *t*-test to determine statistical differences between the two periods. To confirm these differences, Fisher's LSD post hoc test was applied. Finally, a linear regression analysis was performed to show the relationship between the temporal NDVI data for each adjacent city and SO_2 concentrations. The results were evaluated using the coefficient of determination (R^2), the MAE, and the *p*-value at a 95% significance level. The statistical analyses were conducted using Statgraphics Centurion 19 and MS Excel.

3. Results

3.1. Trend Analysis Results for SO_2 and NDVI. Figure 3 illustrates the dynamics of SO_2 in the study area during 2005–2019. A general decrease in the concentrations of this pollutant over time is observed. The reduction covers much of the study area,

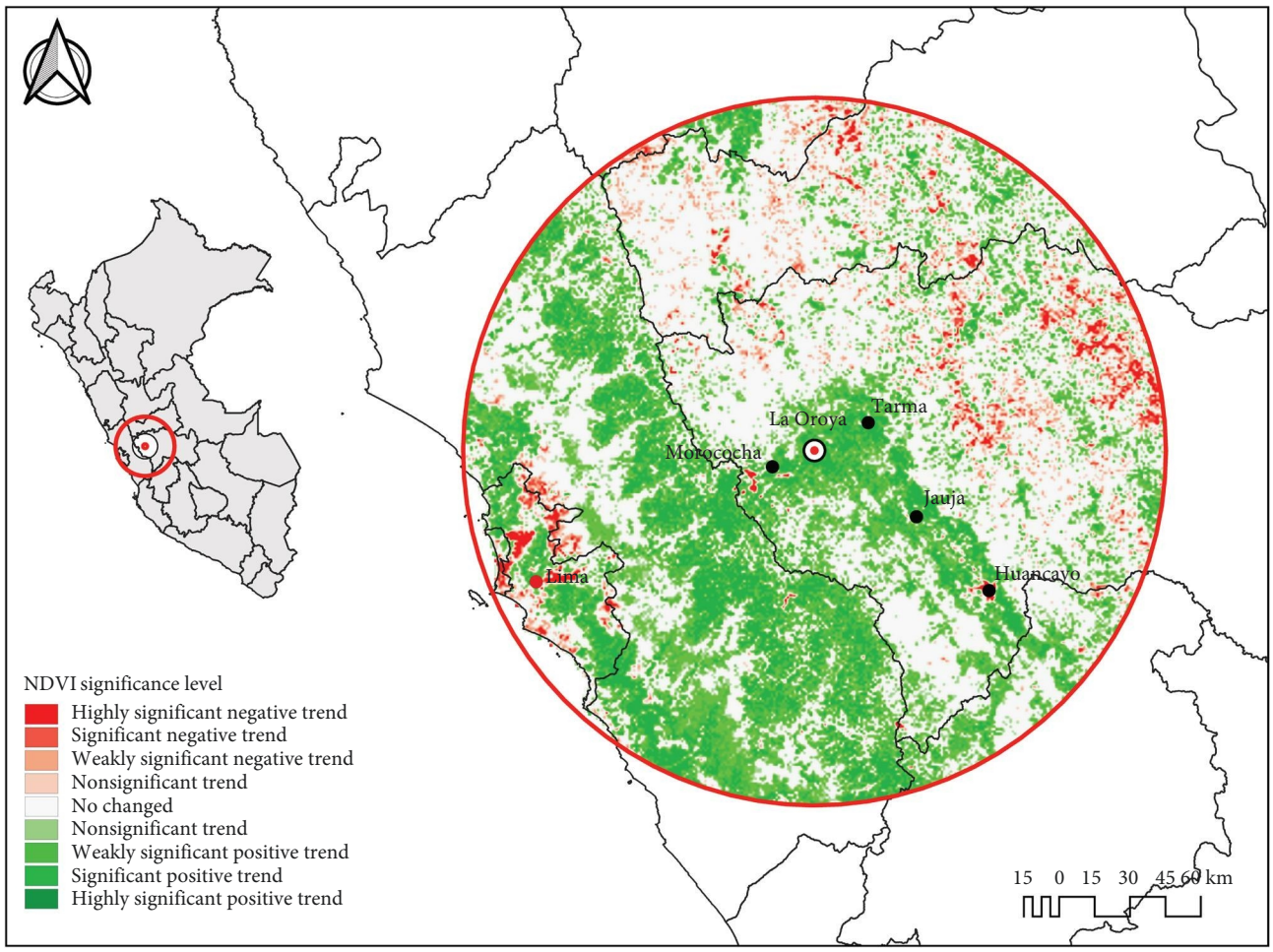

FIGURE 4: NDVI trend significance levels in the study area for 2000–2019.

extending westward towards Lima, the capital of Peru. This pattern is notable as it suggests that SO_2 from the study area may have contributed to the existing pollution levels in Lima. Additionally, the decrease in SO_2 also affects the south, southwest, and southeast, covering regions such as the Mantaro Valley, Huancayo, and part of the Huancavelica department. Conversely, in the northeast, including cities like La Merced, Chanchamayo, and Pichanaki, an increase in SO_2 concentrations is observed. This rise could be related to the growth of vehicle fleets and population increases in these areas [20, 21]. Therefore, SO_2 air pollution has been significant, affecting vast areas and showing notable decreases and increases in nearby cities.

Figure 4 shows the distribution of the NDVI trend for the 2000–2019 period. Vegetation near the cities included in the study demonstrates regeneration during this period. However, in some places, vegetation degradation is observed, attributed to changes in land use due to mining, urbanization, and other economic activities such as agriculture and grazing. Moreover, vegetation recovery is primarily oriented towards the southeast, south–southwest, and west from the location of the CMLO. This regeneration orientation coincides with the direction of SO_2 dispersion, as shown in Figure 3, suggesting that vegetation regeneration patterns may be influenced by prevailing wind directions carrying SO_2.

3.2. Time Series Results. The time series presented in Figure 4 is divided into four segments, each analyzing different aspects. The first segment (Figure 5a) focuses on average SO_2 levels, while the subsequent segments (Figure 5b–d) examine NDVI in various adjacent cities. For both datasets, two time periods were considered: 2005–2009 (for SO_2), 2000–2009 (for NDVI), and 2010–2019 (for both variables), to compare conditions before and after the CMLO shutdown.

In the first segment of the SO_2 analysis for the 2005–2009 period, elevated levels with high variability are observed, reaching a maximum of 0.407 DU. Despite the high levels, the trend is negative and significant according to the Mann–Kendall test ($p < 0.001$), indicating a gradual decrease in SO_2 levels. Likewise, the second period (2010–2019) shows low variability and significantly reduced SO_2 levels, with a maximum of 0.341 DU and minimum values close to 0 DU. When evaluating the differences between the averages of the first period, 2005–2009 (0.161 DU), and the second period, 2010–2019 (0.028 DU), a decrease of 82.18% is observed. This last period's trend is insignificant ($p > 0.05$), suggesting

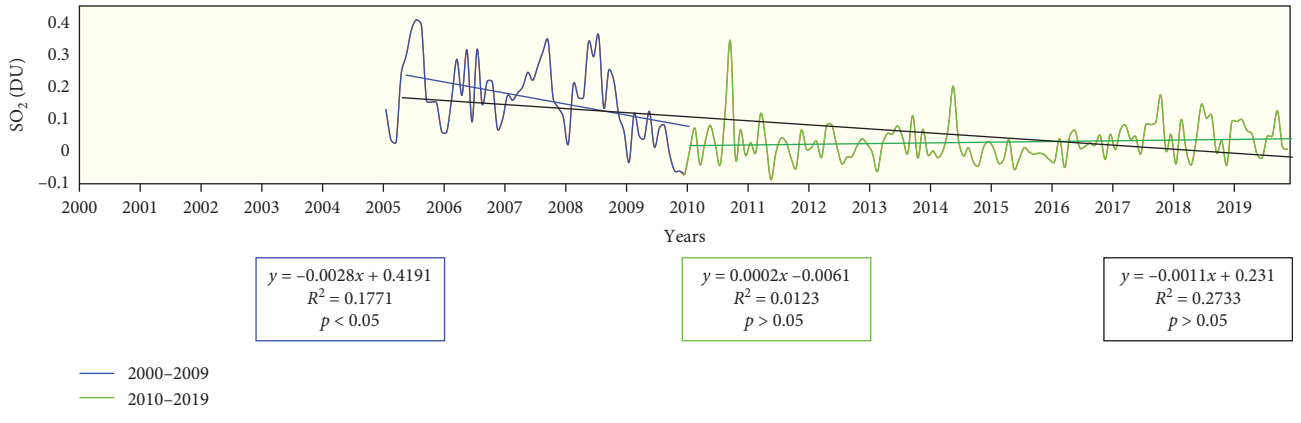

(a)

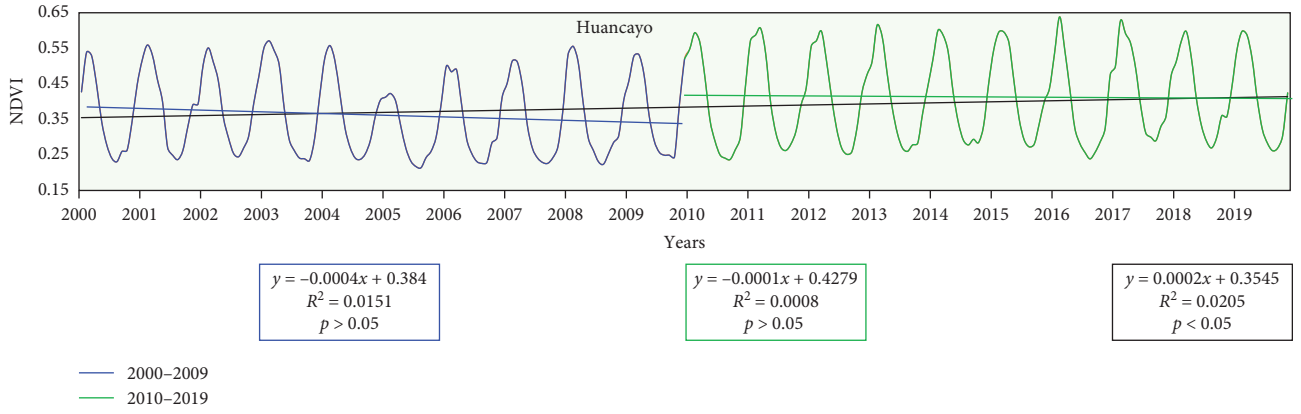

(b)

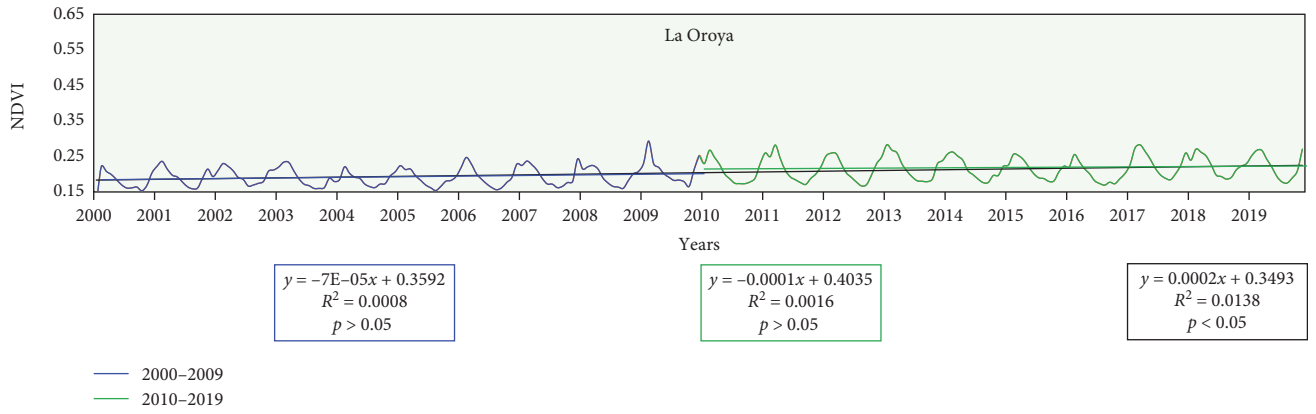

(c)

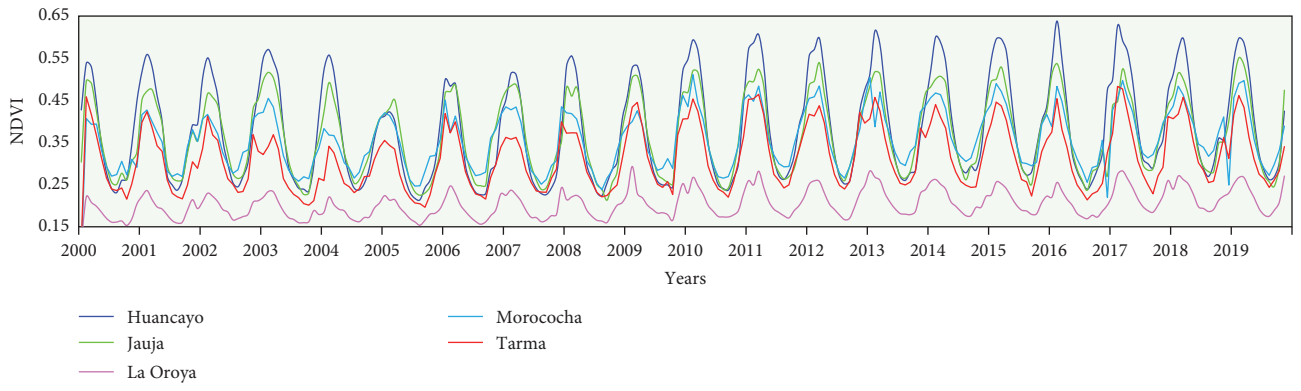

(d)

FIGURE 5: SO_2 and NDVI time series analysis. Temporal trend of SO_2 before and after the CMLO shutdown during the 2005–2019 period (a). Temporal trend of NDVI in adjacent cities before and after the CMLO shutdown during the 2000–2019 period (b–d).

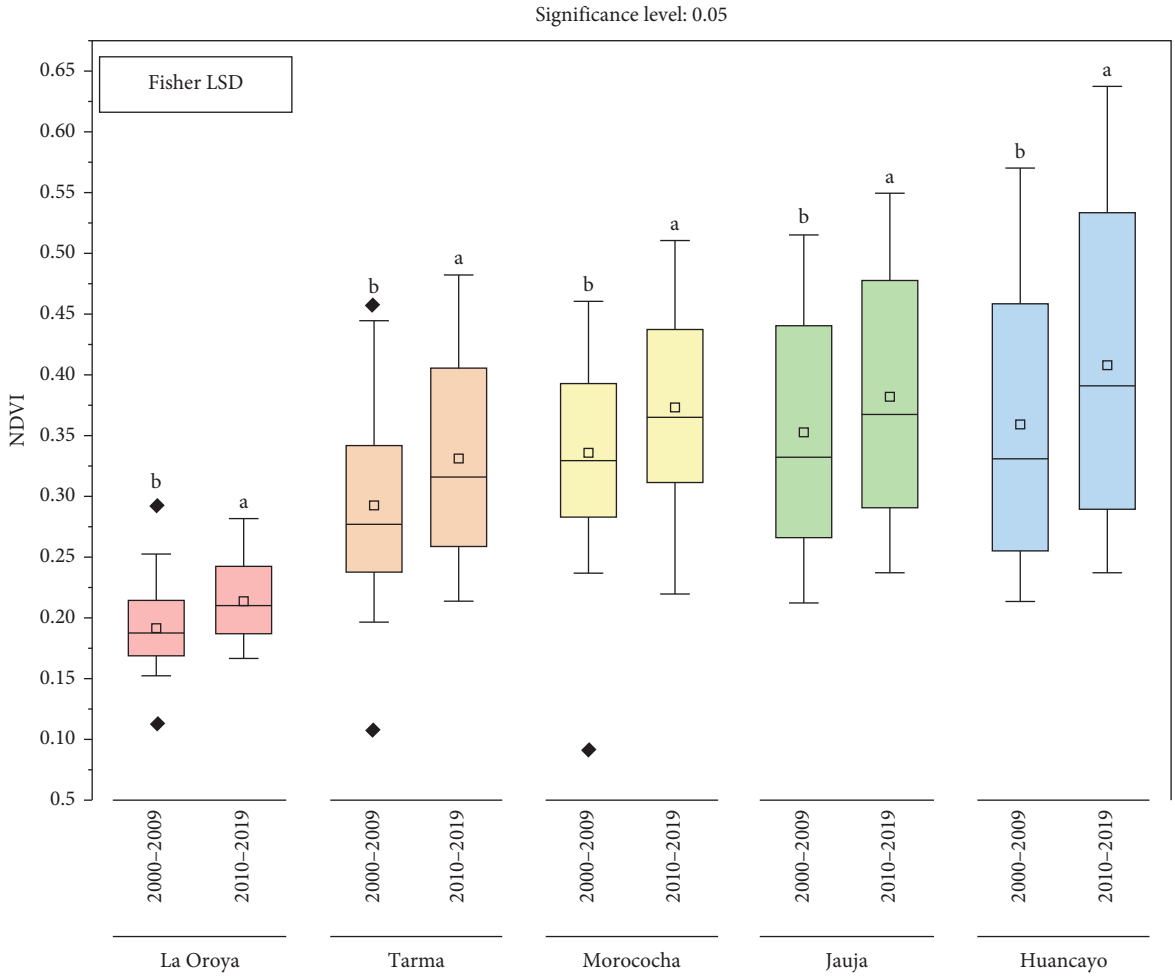

FIGURE 6: NDVI data assessment using box plots for mean NDVI comparisons for the 2000–2009 and 2010–2019 periods before and after the CMLO shutdown. The box plot illustrates data distribution, with interquartile ranges represented by the box. Upper and lower vertical lines indicate maximum and minimum values, respectively. The central line within the box marks the average value, while points outside the box indicate outliers. Different lowercase letters indicate statistically significant differences ($p < 0.05$) according to Fisher's LSD post hoc test.

that SO_2 levels remained low. However, when analyzing the entire 2005–2019 period, the trend is highly significant and negative ($p < 0.001$), reflecting the substantial impact of the CMLO shutdown.

In the NDVI analysis, segments in Figure 5b–d presents the data for different cities: Huancayo (with high NDVI levels), La Oroya (with low NDVI levels), and a composite to observe NDVI across all cities. This segmentation allows for comparisons of NDVI behavior in different contexts, revealing variations in vegetation. For both Huancayo and La Oroya, as well as for the other cities, the analyses were conducted in 2000–2009 and 2010–2019. In neither period were significant NDVI trends found ($p > 0.05$). However, when combining both periods (2000–2019), a statistically significant trend is observed according to the Mann–Kendall test, indicating a clear relationship between the increase in NDVI and the decrease in SO_2. Furthermore, a preliminary analysis of the average of all cities studied in the time series shows an increase from 0.306 to 0.343 between the two periods evaluated. This suggests that the CMLO shutdown had a positive effect on vegetation regeneration. Additionally, Figure 4d shows the NDVI behavior in all cities. While a decrease in NDVI levels is observed as proximity to the CMLO increases, the overall variation pattern overtime is similar to that observed in Huancayo and La Oroya, confirming consistent differences and similarities in NDVI among the studied cities.

Figure 6 illustrates differences in mean NDVI for the two time periods across all time series in cities near the CMLO. Cities are ordered from lowest to highest NDVI levels and by their distance from the CMLO. In all cities, differences between the two periods (2000–2009 and 2010–2019) are statistically significant according to the Student's t-test ($p < 0.05$) and Fisher's LSD multiple range test, as indicated by distinct lowercase letters to emphasize differences at the top of each box plot. These differences confirm that the reduction in SO_2 levels following the CMLO shutdown has notably impacted vegetation regeneration in adjacent areas.

Figure 7 shows the relationship between SO_2 and NDVI in each city adjacent to the CMLO. Results indicate a significant relationship in all studied cities ($p < 0.05$), although this relationship diminishes as the distance from the CMLO increases. This is reflected in the determination coefficients (R^2) for each

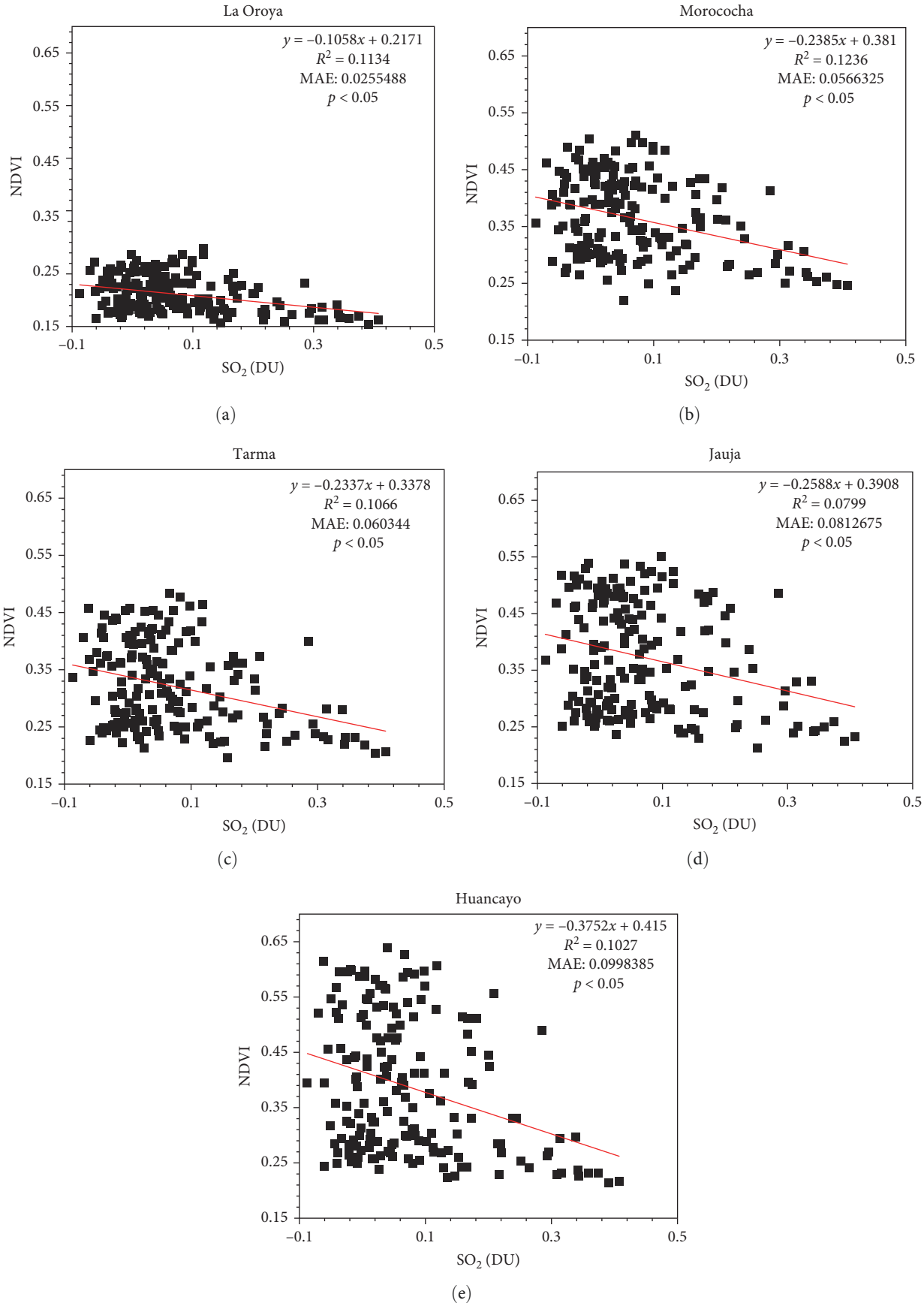

FIGURE 7: Linear regression analysis showing the relationship between NDVI and SO_2 in cities adjacent to the CMLO: La Oroya (a), Morococha (b), Tarma (c), Jauja (d), and Huancayo (e). The red line represents the fitted linear regression. R^2 is the coefficient of determination, MAE is the mean absolute error, and $p<0.05$ indicates a statistically significant relationship.

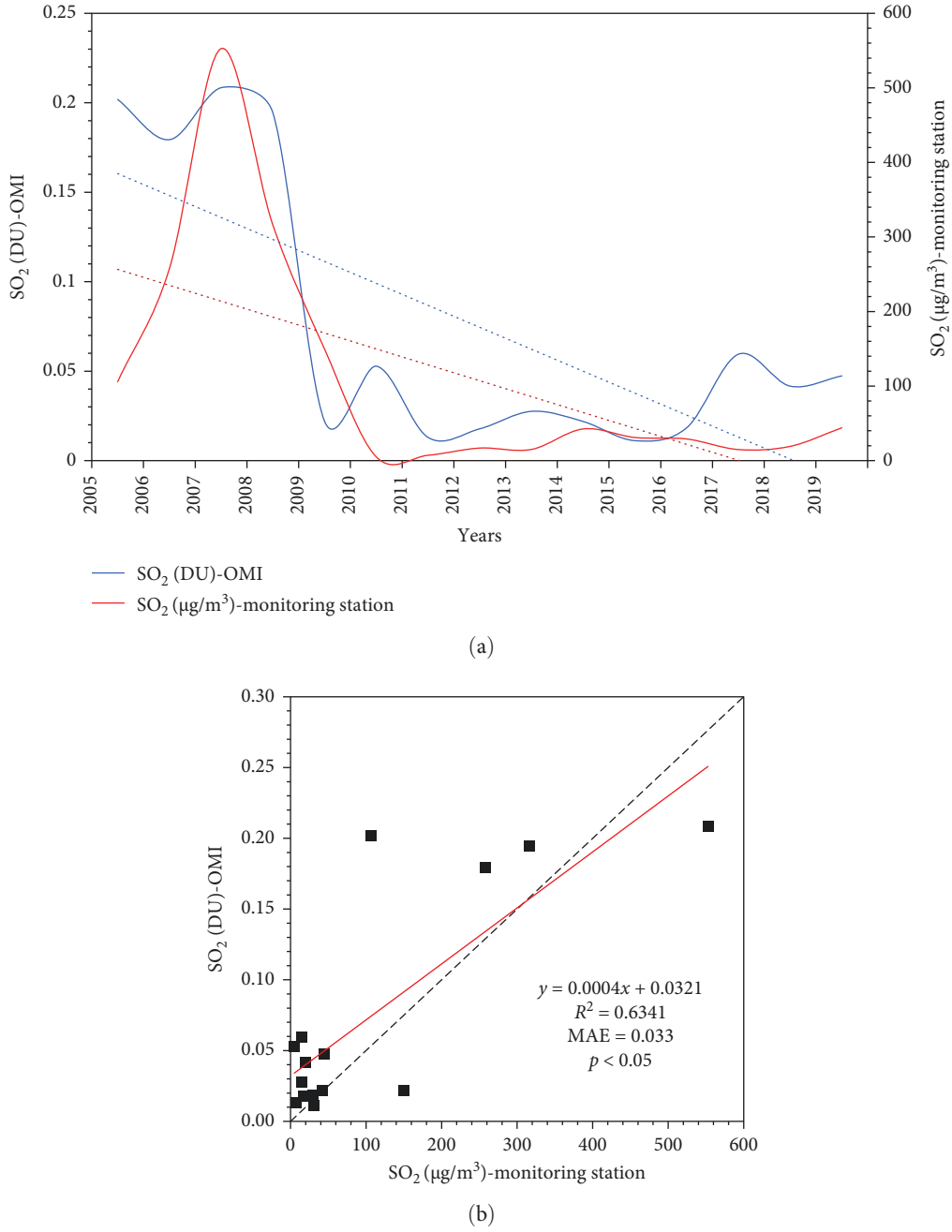

FIGURE 8: Validation of SO_2 data obtained from the OMI sensor, through monitoring data collected in public spaces near the CMLO. (a) Temporal analysis of annual averages from both monitoring sources. Dashed lines correspond to temporal trend lines. (b) Linear regression analysis and the coefficient of determination between the two datasets.

city, with Morococha showing the highest relationship ($R^2 = 0.12$) and Jauja the lowest ($R^2 = 0.07$). Moreover, the MAE also increases with distance from the CMLO. La Oroya recorded the lowest MAE (0.02) and the least data dispersion, while Huancayo exhibited the highest MAE (0.09) and the greatest dispersion. These results suggest a negative relationship between NDVI and SO_2, demonstrating the complex interaction between the reduction of this pollutant and vegetation regeneration in surrounding areas due to the CMLO shutdown.

3.3. Relationship Between Field SO_2 Data and OMI SO_2 Data. To complement the findings of this study, the temporal dynamics of SO_2 DU obtained from the OMI satellite sensor were analyzed together with field measurements of SO_2 in $\mu g/m^3$ taken in urban public spaces near the CMLO (Figure 8a). In both datasets, a sharp and marked decrease in SO_2 levels can be observed, with a notable and sustained change starting in 2009, when the CMLO ceased operations, which is evident in both sources of information. Likewise, when evaluating the statistical relationship between both

sources, a coefficient of determination of $R^2 = 0.63$ was obtained (Figure 6b), with a statistical significance level of $p < 0.05$, indicating a moderate–high and statistically significant relationship. However, some potential biases were identified that could imply overestimations or underestimations by the OMI sensor compared to in situ measurements (MAE = 0.033). These results support the overall consistency between the satellite and field data, allowing us to state that the OMI sensor represents a reliable tool for monitoring SO_2 in this region. Furthermore, the identified patterns are consistent with those presented in the previous results sections, adequately reflecting the temporal evolution of the pollutant in the analyzed period.

3.4. Analysis of Wind Direction and Flow in Nearby Cities. The analyses are complemented by wind rose results with flow vectors indicating wind direction and speed recorded during 2019, corroborating the dispersion of SO_2 pollutants emitted by the CMLO. Figure 9 shows the wind behavior in cities near the CMLO, including Morococha, Tarma, Jauja, and Huancayo. All of them present a predominant wind direction from northeast to southwest. In most of these cities, winds in that sector were recorded between 16% and 24% of the time, with speeds ranging from 0.50 to 8.80 m/s. Likewise, although the same speed range is maintained in Huancayo, this condition occurs less frequently, between 8% and 16% of the time. This atmospheric dynamic suggests that, although SO_2 emissions reach nearby urban areas, most pollutants are dispersed mainly toward the southwest, consistent with the wind patterns observed in previous SO_2 and NDVI trend analyses.

Likewise, temporal evaluations of wind roses with wind flow vectors were carried out for the years 2001 and 2009, in the city of La Oroya and nearby cities (Morococha, Tarma, Jauja, and Huancayo), without finding significant differences between the two periods. Similarly, when comparing conditions between dry and rainy months, no relevant variations were identified. However, when analyzing the differences between day and night in those same years, marked contrasts were observed: during the day, the direction, flow, and speed of the wind were notably greater, while at night, minimal values were recorded. These differences are explained by daily temperature changes, which directly influence atmospheric pressure (Figure 2).

4. Discussions

Remote sensing tools, such as MODIS and OMI sensors, have proven highly effective in assessing environmental impact over extensive and hard-to-reach areas, such as the vicinity of the CMLO. In this study, data from the NDVI provided by MODIS and SO_2 concentrations captured by OMI allowed for identifying spatial and temporal patterns. The accuracy of MODIS data at a 1 km^2 scale, thanks to the MAIAC algorithm, has been globally validated with a correlation coefficient above 0.95 and an RMSE below 0.250 cm [22]. This capability enabled the evaluation of vegetation regeneration, where an average NDVI increase from 0.34 to 0.41 was observed during the postsuspension period of industrial activities. Complementarily, the OMI sensor data were fundamental for monitoring the vertical column densities of SO_2, showing an average decrease of 0.132 DU between 2005–2009 and 2010–2019. This trend coincides with and correlates to the monitoring records of DIRESA ($R^2 = 0.63$), which supports the information obtained through remote sensing about atmospheric pollutants and their effects on local vegetation [23, 24]. These results highlight the advantages of integrating remote sensing technologies with field monitoring efforts, providing a comprehensive view of the environmental dynamics in La Oroya and showing how industrial activities affect air quality and vegetation health.

The average reduction of SO_2 observed in this study was 82.18% (from 0.161 to 0.028 DU) during the postsuspension period of CMLO. This decrease is minor compared to other similar interventions globally. For example, the closure of the ASARCO smelter in the Cascade Lakes region resulted in an 86.2% reduction in SO_2 emissions (from 87 to 12 kilotons per year), demonstrating a substantial improvement in surrounding environmental quality [25]. Similarly, in Newcastle, Australia, the closure of the BHP Rod and Bar steelworks led to a 40.2% decrease in SO_2 concentrations, showing the direct impact of industrial shutdowns on air quality improvements [26]. From a policy perspective, in Beijing, stringent government policies achieved an 81% reduction in SO_2 concentrations between 2013 and 2018, emphasizing the effectiveness of regulatory measures in highly industrialized urban areas [27]. Even temporary shutdowns during the COVID-19 lockdown in northern China reduced SO_2 emissions by an average of 20.1% [28]. Similarly, in the city of Lecce in southeastern Italy, a 64% reduction in ultrafine particle concentration in suburban areas was reported, due to the reduction of vehicular traffic to zero during the lockdown [29], with very similar effects on the SO_2 reduction recorded in La Oroya.

Analysis of the relationship between SO_2 reduction and vegetation recovery indicates that suspending the CMLO activities significantly reduced SO_2 emissions. This pattern suggests a direct link between pollutant reduction and the observed vegetation regeneration in the region. This finding aligns with previous studies, such as in Sudbury, Canada, where SO_2 reduction enabled the recolonization of lichens and partial regeneration of severely damaged areas, although over long timeframes due to the intensity of accumulated damage [30]. Competitive inhibition of ribulose bisphosphate carboxylase and disruption of CO_2 fixation, attributed to the formation of compounds such as α-hydroxy sulfonate, demonstrate how SO_2 directly affects essential metabolic processes for photosynthesis [31, 32]. In this context, the improvement of the NDVI in La Oroya and surrounding cities, with an average increase from 0.306 to 0.343 between the two evaluated periods, reflects the progressive restoration of the photosynthetic and metabolic capacity of the vegetation, favoring the increase of coverage and its resilience to pollution. Although the absolute NDVI values are relatively low, the recovering areas show a statistically significant temporal trend from 2000 to 2019. Nevertheless, it is important to point out that many plant species in the region present slow growth rates and xerophytic adaptations to survive under conditions of low water availability, which may limit the accumulation of biomass and, consequently, prevent the attainment of high NDVI values [10, 33].

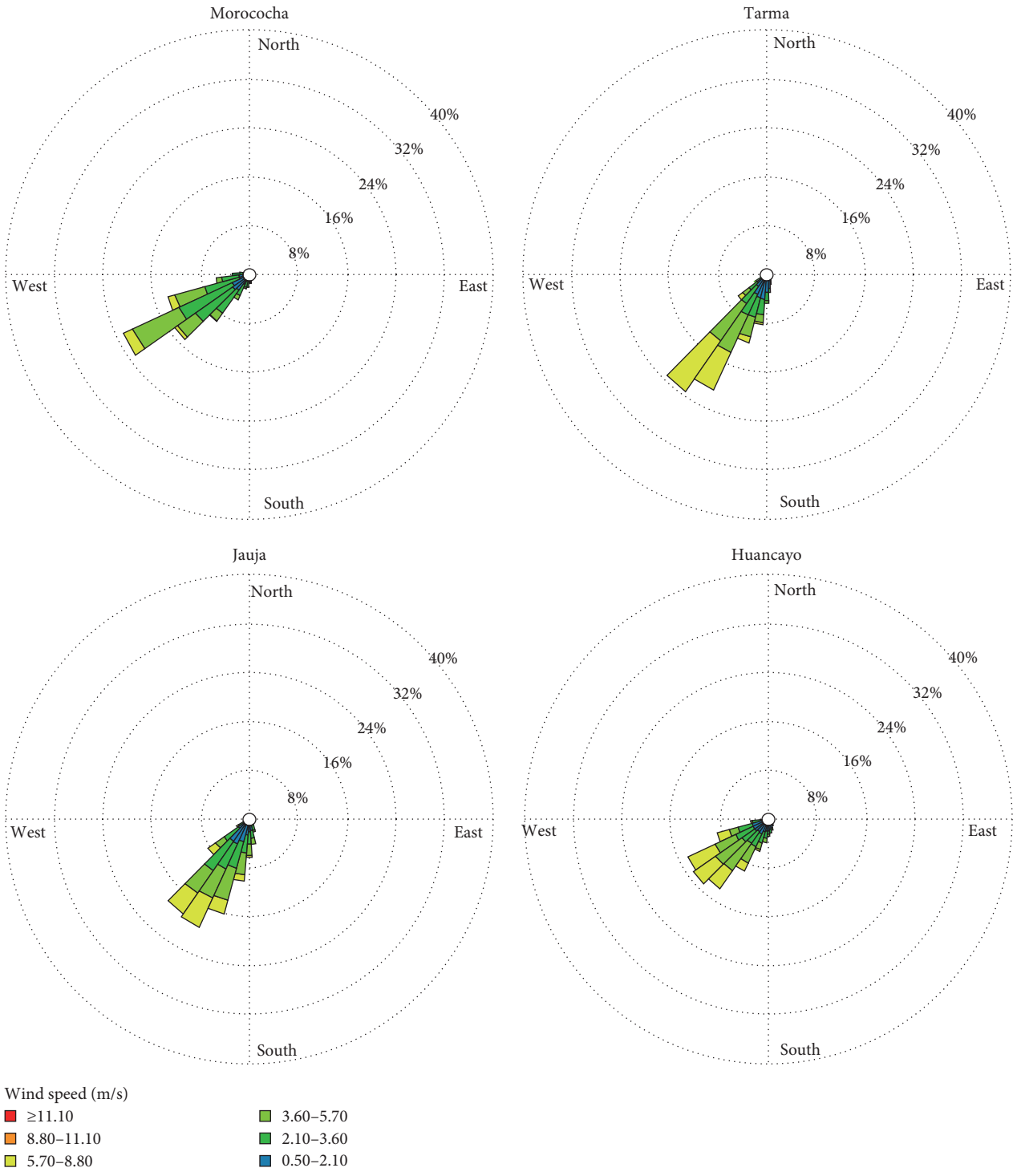

Figure 9: Wind rose with flow vectors indicating the direction toward which the wind is moving and its speed in the cities surrounding the CMLO.

This increase in NDVI is comparable with studies from Great Britain, where reductions in sulfur improved soil pH by 0.2 units, which favored changes in plant composition in low-intensity areas [34], due to the decrease in acidification with the reduction in sulfuric acid formation [35]. However, the vegetation response in La Oroya highlights local species' heterogeneity and susceptibility to SO_2. In particular, lichens, as biological indicators sensitive to SO_2, are highly affected by the absorption of this gas, which can become toxic compounds such as bisulfite and sulfite, negatively impacting photosynthesis and respiration [36, 37]. Although the NDVI showed an average increase from 0.306 to 0.343, this result reflects a partial recovery, in line with studies in mining zones such as El Vinagre in Colombia, where lichen diversity was significantly

lower near sources of SO_2 pollution, indicating that ecosystem recovery may be slower in areas with severe historical damage [38]. The high-Andean vegetation near La Oroya presents unique adaptive characteristics, but its sensitivity to pollution is evident. The grasslands of this region, dominated by species such as *Festuca dolichophylla* and *Stipa ichu*, experienced chemical alterations in the soil due to the historical accumulation of sulfur, which may have affected their structure and productivity [39, 40]. The recovery observed in the NDVI also suggests that, although local conditions still face restrictions derived from water scarcity and soil chemistry, the decrease in SO_2 has allowed gradual regeneration in the less degraded areas.

The analyses show that wind plays a key role in the dispersion of SO_2 in the central Andes. In most studied cities, northeast-to-southwest winds predominate much of the year, a pattern previously reported in the region [1, 41]. These flows favor the transport and distribution of pollutants, especially during daytime hours, when the increase in wind speed, driven by the marked temperature fluctuations between day and night typical of the central Andes, improves their dispersal capacity [42]. Warmer daytime temperatures generate atmospheric instability, modifying pressure gradients and increasing wind speed, facilitating pollutants' dispersion toward the southwest [43]. Likewise, nighttime cooling stabilizes the atmosphere and can trap pollutants near the surface [44], which would explain their accumulation and eventual transport toward cities located opposite the predominant flow, such as Tarma, Jauja, and Huancayo. This behavior generates marked differences in pollutant concentrations depending on the day. It highlights the importance of meteorological factors, particularly wind speed and direction, in the region's air quality dynamics. Taken together, the results suggest that a large part of the pollutants emitted by the CMLO reach these cities at night, while during the day they are mainly dispersed toward the southwest.

The spatial distribution of regeneration in the study area highlights more notable recovery toward the southwest and southeast of CMLO, reflecting the influence of prevailing winds on SO_2 dispersion. Specific wind directions and seasonal variations have been crucial in this pollutant's deposition. Studies have shown that high wind speeds can dilute SO_2 concentrations, while their direction can transport pollutants to more distant regions, altering the patterns of vegetation damage and recovery [45]. This phenomenon is consistent with observations in central Taiwan, where SO_2 concentrations are higher in winter due to the transport of emissions by prevailing wind patterns [46]. In La Oroya, these dynamics could explain why areas in the wind trajectories to the southwest and southeast show faster recovery, while regions closer to CMLO, exposed to more concentrated deposits, exhibit slower regeneration.

However, plants' ability to absorb SO_2 and reduce their atmospheric concentration depends on factors such as aerodynamic resistance and meteorological conditions, which can influence deposition and recovery rates. This behavior aligns with findings in Alberta, Canada, where sulfur reductions significantly increased the productivity of species such as lodgepoles and jackpines [47]. In the Central Appalachian Mountains, a similar dynamic was observed following the implementation of the Clean Air Act, where species like *Juniperus virginiana* improved photosynthesis and stomatal conductance as pollution decreased [48].

In contrast to global precedents, the relationship between SO_2 reduction and NDVI in the study area presented moderate determination coefficients, averaging $R^2 = 0.10$. This value suggests a weaker relationship than in settings where pollutant reductions have resulted in faster and more homogeneous recovery, such as highly polluted urban areas that have reported significant increases in vegetation biomass [49]. This behavior can be partially explained by the complex dynamics affecting vegetation health and the accuracy of vegetation indices in diverse environmental conditions. Studies have shown that SO_2 directly impacts plant health by reducing chlorophyll concentrations. In rice canopy experiments, SO_2 concentrations showed a strong negative relationship with chlorophyll a, chlorophyll b, and total chlorophyll, with correlation coefficients ranging from −0.454 to −0.618, indicating significant effects on photosynthetic mechanisms [50].

5. Conclusions

This study has highlighted the positive impact of suspending activities at the CMLO on air quality and vegetation regeneration in surrounding areas. The average reduction of SO_2 by 82.18% during the analysis period (2005–2019) was accompanied by a significant recovery of vegetation according to the Mann–Kendall trend analysis of the NDVI in the period 2000–2019, in areas that were affected by SO_2 pollution. These results confirm that decreasing atmospheric pollutants can facilitate the recovery of degraded ecosystems, especially in areas of high ecological vulnerability such as high-Andean grasslands. Likewise, the spatial orientation of regeneration, influenced by wind patterns and SO_2 deposition, underscores the importance of local conditions in recovery dynamics.

However, the study also identified certain limitations. The moderate relationship between the reduction of SO_2 and the NDVI ($R^2 = 0.10$) reflects the complexity of interactions between air pollution, soil characteristics, and vegetation regeneration. This suggests that additional factors, such as the historical accumulation of heavy metals, water scarcity, and the specific plant species composition, may play a crucial role in the ecosystem response. Moreover, the spatial resolution of the tools used could limit the detection of finer changes in vegetation, especially in highly fragmented areas. Future research could focus on integrating data from higher-resolution remote sensors.

This study underscores the positive impact on vegetation regeneration associated with SO_2 reduction, a well-known atmospheric pollutant with devastating environmental effects. The decrease in SO_2 has facilitated vegetation regeneration over the years in areas adjacent to CMLO. The utility of remote sensors for conducting macrolevel analyses and assessing ecosystem health following events such as CMLO activity suspension is confirmed. Temporal and spatial trend analysis using the Mann–Kendall method has proven effective in understanding

the relationship between SO_2 reduction and vegetation regeneration. Despite inherent limitations in spatial resolution and missing data, the information provided has been valuable for its level of temporal detail, allowing observation of the dynamics of the variables studied. For a more comprehensive understanding, it would be beneficial to include the analysis of other atmospheric pollutants, such as CO_2 and NO_2, which also affect vegetation health. In the case of CMLO reactivation, the information obtained in this study should be considered for environmental decision-making, recognizing that the addressed issue is closely linked to deeper economic and social aspects, which remain unresolved for achieving sustainable development of this city.

Data Availability Statement

The data supporting this study's findings are available from the corresponding author upon reasonable request.

Ethics Statement

The authors have no relevant information to disclose.

Consent

The authors have no additional information to disclose.

Disclosure

The funding source did not influence the results or their interpretation.

Conflicts of Interest

The authors declare no conflicts of interest.

Funding

This study was funded by the Universidad de Huánuco.

References

[1] J. A. Espinoza-Guillen, M. B. Alderete-Malpartida, J. H. Cañari-Cancho, D. L. Pando-Huerta, D. F. Vargas-La Rosa, and S. J. Bernabé-Meza, "Immission Levels and Identification of Sulfur Dioxide Sources in La Oroya City, Peruvian Andes," *Environment, Development and Sustainability* 25, no. 11 (2023): 12843–12872.

[2] H. E. Ling-Yun and O. U. Jia-Jia, "Taxing Sulphur Dioxide Emissions: A Policy Evaluation From Public Health Perspective in China," *Energy and Environment* 27, no. 6-7 (2016): 755–764.

[3] W. Yang, Z. He, H. Huang, and J. Huang, "A Clustering Framework to Reveal the Structural Effect Mechanisms of Natural and Social Factors on PM2.5 Concentrations in China," *Sustainability* 13, no. 3 (2021): 1428.

[4] G. Qu, R. Jian, J. Zhang, J. Li, and P. Ning, "Capture of Sulphur Dioxide by Hydroxyl Ammonium Ionic Liquid-DBU Mixtures," *Asian Journal of Chemistry* 26, no. 22 (2014): 7823–7827.

[5] M. E. Koukouli, K. Michailidis, P. Hedelt, et al., "Volcanic SO2Layer Height by TROPOMI/S5P:Evaluation Against IASI/MetOp and CALIOP/CALIPSO Observations," *Atmospheric Chemistry and Physics* 22, no. 8 (2022): 5665–5683.

[6] S. A. Abdul-Wahab and B. Yaghi, "Use of Plants to Monitor Contamination of Air by SO2 in and Around Refinery," *Journal of Environmental Science and Health, Part A* 39, no. 6 (2004): 1559–1571.

[7] S. Jha and A. Yadav, "Plants Response to SO_2 or Acid Deposition. Plants and Their Interaction to Environmental Pollution: Damage Detection, Adaptation, Tolerance," *Physiological and Molecular Responses* (2023): 99–108.

[8] C. Xian, T. Wu, J. Liu, and Z. Ouyang, "Air Pollutant Removal by Urban Vegetation: A Meta-Analysis of Gaps in Research and Environmental Management," (2022).

[9] L. Cotrozzi, "Leaf Demography and Growth Analysis to Assess the Impact of Air Pollution on Plants: A Case Study on Alfalfa Exposed to a Gradient of Sulphur Dioxide Concentrations," *Atmospheric Pollution Research* 11, no. 1 (2020): 186–192.

[10] D. Cano, A. Crispin, M. Custodio, F. Chanamé, R. Peñaloza, and S. Pizarro, "Space-Time Quantification of Aboveground Net Primary Productivity Service Supply Capacity in High Andean Bofedales Using Remote Sensors," *Journal of Water and Land Development* 56 (2023): 172–181.

[11] M. Deng, X. Meng, Y. Lu, et al., "The Response of Vegetation to Regional Climate Change on the Tibetan Plateau Based on Remote Sensing Products and the Dynamic Global Vegetation Model," *Remote Sensing* 14, no. 14 (2022): 3337, 2022.

[12] M. K. Reuer, N. W. Bower, J. H. Koball, et al., "Lead, Arsenic, and Cadmium Contamination and Its Impact on Children's Health in La Oroya, Peru," *ISRN Public Health* 2012 (2012): 1–12.

[13] A. Mendiola, C. Aguirre, •. Carla, P. Carpio, V. Monroy, and Y. Paredes, "Perspectivas de reestructuración del Complejo Metalúrgico de La Oroya mediante un análisis ambiental y económico," 2017, https://hdl.handle.net/20.500.12640/1220.

[14] J. C. Bedriñana, D. C. Peinado, and R. Peñaloza-Fernández, "Lead Bioaccumulation in Root and Aerial Part of Natural and Cultivated Pastures in Highly Contaminated Soils in Central Andes of Peru," *Advances in Science, Technology and Engineering Systems Journal* 5, no. 2 (2020): 126–132.

[15] Diario Oficial El Peruano, "Complejo Metalúrgico de La Oroya Reinició Operaciones tras 13 años de paralización," 2023, https://www.elperuano.pe/noticia/225649-complejo-metalurgico-de-la-oroya-reinicio-operaciones-tras-13-anos-de-paralizacion.

[16] A. Meza, "Informe Jurídico sobre la Sentencia de la Corte Interamericana de Derechos Humanos respecto al Caso Habitantes de La Oroya vs. Perú" 2024, https://tesis.pucp.edu.pe/repositorio//handle/20.500.12404/28445.

[17] D. R. Helsel and L. M. Frans, "Regional Kendall Test for Trend," *Environmental Science and Technology* 40, no. 13 (2006): 4066–4073.

[18] W. Sun, H. Song, X. Yao, H. Ishidaira, and Z. Xu, "Changes in Remotely Sensed Vegetation Growth Trend in the Heihe Basin of Arid Northwestern China," *PLOS ONE* 10, no. 8 (2015): e0135376.

[19] D. Cano, C. Cacciuttolo, C. Rosario, et al., "Performance of Green Areas in Mitigating the Alteration of Land Surface Temperature in Urban Zones of Lima, Peru," *Remote Sensing* 17, no. 8 (2025): 1323.

[20] J. Angeles Suazo, R. Angeles Vasquez, E. Y. Chavarría Márquez, et al., "Evaluation of Air Quality by Particulate Matter in Junin and Huancavelica, Peru," *Nature Environment and Pollution Technology* 24, no. 2 (2025): D1722.

[21] G. Sharmilaa and T. Ilango, "A Review on Influence of Age of Vehicle and Vehicle Traffic on Air Pollution Dispersion," *Materials Today: Proceedings* 60 (2022): 1629–1632.

[22] V. S. Martins, A. Lyapustin, Y. Wang, et al., "Global Validation of Columnar Water Vapor Derived From EOS MODIS-MAIAC Algorithm Against the Ground-Based AERONET Observations," *Atmospheric Research* 225 (2019): 181–192.

[23] M. S. Johnson, A. H. Souri, S. Philip, et al., "Satellite Remote-Sensing Capability to Assess Tropospheric-Column Ratios of Formaldehyde and Nitrogen Dioxide: Case Study During the Long Island Sound Tropospheric Ozone Study 2018 (LISTOS 2018) Field Campaign," *Atmospheric Measurement Techniques* 16, no. 9 (2023): 2431–2454.

[24] C. Viatte, C. Clerbaux, C. Maes, et al., "Air Pollution and Sea Pollution Seen From Space," *Surveys in Geophysics* 41, no. 6 (2020): 1583–1609.

[25] E. B. Welch, D. E. Spyridakis, K. B. Easthouse, T. J. Smayda, and L. C. Duncan, "Response to a Smelter Closure in Cascade Mountain Lakes," *Water, Air, and Soil Pollution* 61, no. 3-4 (1992): 325–338.

[26] S. A. Sajjadi, H. Bridgman, and N. Sadeghi, "Changes in Air Quality due to Closure of a Major Industry," *En International Journal of Collaborative Research on Internal Medicine and Public Health* 4 (2012): 1196–1214.

[27] X. Li, B. Zhao, W. Zhou, et al., "Responses of Gaseous Sulfuric Acid and Particulate Sulfate to Reduced SO2 Concentration: A Perspective From Long-Term Measurements in Beijing," *Science of the Total Environment* 721 (2020): 137700.

[28] J. Mo, S. Gong, J. He, L. Zhang, H. Ke, and X. An, "Quantification of SO2 Emission Variations and the Corresponding Prediction Improvements Made by Assimilating Ground-Based Observations," *Atmosphere* 13, no. 3 (2022): 470.

[29] A. Donateo, A. Dinoi, and G. Pappaccogli, "Impact on Ultrafine Particles Concentration and Turbulent Fluxes of SARS-CoV-2 Lockdown in a Suburban Area in Italy," *Atmosphere* 12, no. 3 (2021): 407.

[30] J. Gunn, W. Keller, J. Negusanti, R. Potvin, P. Beckett, and K. Winterhalder, "Ecosystem Recovery After Emission Reductions: Sudbury, Canada," *Water, Air, and Soil Pollution* 85, no. 3 (1995): 1783–1788.

[31] S. S. Malhotra and D. Hocking, "Biochemical and Cytological Effects of Sulphur Dioxide on Plant Metabolism," *New Phytologist* 76, no. 2 (1976): 227–237.

[32] H. Tanaka, T. Takanashi, and M. Yatazawa, "Experimental Studies on Sulfur Dioxide Injuries in Higher Plants," *Water, Air, and Soil Pollution* 1, no. 2 (1972): 205–211.

[33] L. A. Duffaut Espinosa, A. N. Posadas, M. Carbajal, and R. Quiroz, "Multifractal Downscaling of Rainfall Using Normalized Difference Vegetation Index (NDVI) in the Andes Plateau," *PLOS ONE* 12, no. 1 (2017): e0168982.

[34] F. M. Seaton, D. A. Robinson, D. Monteith, et al., "Fifty Years of Reduction in Sulphur Deposition Drives Recovery in Soil PH and Plant Communities," *Journal of Ecology* 111, no. 2 (2023): 464–478.

[35] Q. Yu, T. Zhang, X. Ma, et al., "Monitoring Effect of SO2 Emission Abatement on Recovery of Acidified Soil and Streamwater in Southwest China," *Environmental Science and Technology* 51, no. 17 (2017): 9498–9506.

[36] V. I. Deltoro, C. Gimeno, A. Calatayud, and E. Barreno, "Effects of SO2 Fumigations on Photosynthetic CO2 Gas Exchange, Chlorophyll a Fluorescence Emission and Antioxidant Enzymes in the Lichens *Evernia prunastri* and *Ramalina farinacea*," *Physiologia Plantarum* 105, no. 4 (1999): 648–654.

[37] T. Nash Iii and C. Gries, "Lichens as Bioindicators of Sulfur Dioxide," *En Symbiosis* 33 (2002): 1–21.

[38] D. D. Escandón, E. S. Medina, R. Lücking, and P. A. S. Sopkin, "Corticolous Lichens as Environmental Indicators of Natural Sulphur Emissions Near the Sulphur Mine El Vinagre (Cauca, Colombia)," *The Lichenologist* 48, no. 2 (2016): 147–159.

[39] H. Ejaz, E. Bibi, W. Ali, et al., "Sulphur and Particulate Matter Affecting on Soil and Underground Plants," *Journal of Agriculture and Applied Biology* 3, no. 1 (2021): 40–49.

[40] D. Cano, S. Pizarro, C. Cacciuttolo, R. Peñaloza, R. Yaranga, and M. L. Gandini, "Study of Ecosystem Degradation Dynamics in the Peruvian Highlands: Landsat Time-Series Trend Analysis (1985-2022) With ARVI for Different Vegetation Cover Types," *Sustainability* 15, no. 21 (2023): 15472.

[41] J. Ulloa Ninahuamán, D. Alvarez-Tolentino, A. Peña Rojas, et al., "Sensores de bajo costo en la caracterización de partículas finas (PM2.5) de una ciudad altoandina," *Revista de Investigaciones Altoandinas - Journal of High Andean Research* 24, no. 3 (2022): 199–207.

[42] T. O. Roomi and A. S. Abed, "Estimating Gaseous Pollutants in the Air Near Daura Refinery, Daura Power Plant and South of Baghdad Power Plant by Calculating the Fuel Discharge," *Scientific Review Engineering and Environmental Studies (SREES)* 30, no. 1 (2021): 195–207.

[43] R. Estevan, D. Martínez-Castro, L. Suarez-Salas, A. Moya, and Y. Silva, "First Two and a Half Years of Aerosol Measurements With an AERONET Sunphotometer at the Huancayo Observatory, Peru," *Atmospheric Environment: X* 3 (2019): 100037.

[44] D. Giosanu, M. C. Marian, and A. Zaharia, "The Influence of Meteorological and Topographical Parameters on the Dispersion of PM10 and CO Pollutants," *Current Trends in Natural Sciences* 10, no. 19 (2021): 92–98.

[45] C. Talbot, C. Leroy, P. Augustin, et al., "Transport and Dispersion of Atmospheric Sulphur Dioxide From an Industrial Coastal Area During a Sea-Breeze Event," *Atmospheric Chemistry and Physics Discussions* 7, no. 6 (2007): 15989–16022.

[46] N. Cheng, D. Zhang, Y. Li, et al., "Analysis About Spatial and Temporal Distribution of SO2 and An Ambient SO2 Pollution Process in Beijing During 2000-2014," *Huan Jing Ke Xue = Huanjing Kexue* 36, no. 11 (2015): 3961–3971.

[47] A. H. Legge, M. Nosal, and S. V. Krupa, "Modeling the Numerical Relationships Between Chronic Ambient Sulphur Dioxide Exposures and Tree Growth," *Canadian Journal of Forest Research* 26, no. 4 (1996): 689–695.

[48] R. B. Thomas, S. E. Spal, K. R. Smith, and J. B. Nippert, "Evidence of Recovery of *Juniperus virginiana* Trees From Sulfur Pollution Sfter the Clean Air Act," *Proceedings of the National Academy of Sciences* 110, no. 38 (2013): 15319–15324.

[49] N. A. Hassan, Z. Hashim, and J. H. Hashim, "Impact of Climate Change on Air Quality and Public Health in Urban Areas," *Asia Pacific Journal of Public Health* 28, no. 2_suppl (2016): 38S–48S.

[50] J. Zhang, C. Han, and Y. Li, "The Effects of Sulphur Dioxide on the Spectral Curves and Chlorophyll Concentration of Rice Canopy," *International Journal of Remote Sensing* 31, no. 16 (2010): 4257–4264.